METRIC/INCH-POUND

KSC-STD-Z-0017
MAY 8, 2014

ENGINEERING ANALYSIS, THERMAL/FLUID, STANDARD FOR

ENGINEERING AND TECHNOLOGY DIRECTORATE

National Aeronautics and
Space Administration

John F. Kennedy Space Center

KSC FORM 16-12 (REV. 6/95) PREVIOUS EDITIONS ARE OBSOLETE (CG 11/95)

NASA KSC Export Control Office (ECO)
Export/SBU Determination Record

EDDR# 128965

DOCUMENT INFORMATION: (TITLE, NUMBER, REV, DATE)
KSC-STD-Z-0017 ENGINEERING ANALYSIS, THERMAL/FLUID, STANDARD FOR

SENSITIVE BUT UNCLASSIFIED (SBU)

INSTRUCTIONS: This item must be reviewed under the requirements for "Sensitive But Unclassified Information" as described in NPR 1600.1, Chapter 5.

http://nodis-dms.gsfc.nasa.gov

	Yes	*No*	*SBU Reviewer's Signature*	*Date*	*Company / Org*
Document contains SBU?	☐	☒	Chasity Harvey (affiliate) (11/15/2012)	11/15/2012	ESC

EXPORT CONTROL (EC)

INSTRUCTIONS: Attach the document requiring an export determination. Contact the KSC ECO Help Desk (867-9209) for help in completing this form.

http://exportcontrol.ksc.nasa.gov/

Contractor EC Reviewer's Name and Organization	*Contractor EC Reviewer's Signature*	*Date*
CHASITY HARVEY ESC	Chasity Harvey (affiliate) (11/15/2012)	11/15/2012
NASA ECO Reviewer's Name and Organization	*NASA ECO Reviewer's Signature*	*Date*
TA-A5A	DOUGLAS LESHO (11/15/2012)	

	EXPORT DETERMINATION *(Check one box only)*	
EAR 99	☒ **NLR**	The information contained in the document is technical in content, but is not technical data as defined by the ITAR or the EAR, and therefore is EAR 99 NLR (no export license required). [General Prohibition Six (Embargo) applies to all items subject to the EAR, i.e. items on the CCL and within EAR 99 NLR. You may not make an export or re-export contrary to the provisions of part 746 (Embargos and Other Special Controls) of the EAR and 22 CFR part 126.1 of the ITAR.]
EAR Controlled	☐	This document is within the purview of the Export Administration Regulations (EAR), 15 CFR 730-774, and is export controlled. It may not be transferred to foreign nationals in the U.S. or abroad without specific approval of a knowledgeable NASA export control official, and/or unless an export license or license exception is obtained/available from the Bureau of Industry and Security, United States Department of Commerce. Violations of these regulations are punishable by fine, imprisonment, or both.
ITAR Controlled	☐	This document contains information which falls under the purview of the U.S. Munitions List (USML), as defined in the International Traffic in Arms Regulations (ITAR), 22 CFR 120-130, and is export controlled. It shall not be transferred to foreign nationals, in the U.S. or abroad, without specific approval of a knowledgeable NASA export control official, and/or unless an export license or license exemption is obtained/available from the United States Department of State. *Violations of these regulations are punishable by fine, imprisonment, or both.*

KSC FORM 7-657V2 NS (REV. 09/11) PREVIOUS EDITIONS ARE OBSOLETE

METRIC/INCH-POUND

KSC-STD-Z-0017
MAY 8, 2014

ENGINEERING ANALYSIS, THERMAL/FLUID, STANDARD FOR

Approved by:

P.E. Phillips
Director, Engineering and Technology
Directorate

JOHN F. KENNEDY SPACE CENTER, NASA

CONTENTS

FIGURES

TABLES

ABBREVIATIONS, ACRONYMS, AND SYMBOLS

%	percent
°	degree
°C	degree Celsius
°F	degree Fahrenheit
°R	degree Rankine
ANSI	American National Standards Institute
ASME	American Society of Mechanical Engineers
ASTM	American Society for Testing and Materials
atm	atmosphere
Btu	British thermal unit
CAD	computer-aided design
CDR	Critical Design Review
CEA	Chemical Equilibrium with Application
CFD	computational fluid dynamics
DT	design temperature
DWG	drawing
e.g.	for example
ESD	Exploration Systems Development
ft	foot
g	gram
GCI	grid convergence index
GSFC	Robert H. Goddard Space Flight Center
HDBK	handbook
hr	hour
in	inch
IR	infrared
ISA	International Society of Automation
J	joule
K	kelvin
k	kilo ($1 \cdot 10^3$)

KSC	John F. Kennedy Space Center
lb	pound
lb_f	pound force
lb_m	pound mass
m	meter
m	milli ($1 \cdot 10^{-3}$)
MAPTIS	Materials and Processes Technical Information System
Max	maximum
Min	minimum
MLI	multilayered insulation
MNL	manual
mol	molar
MSFC	George C. Marshall Space Flight Center
N	newton
NA	not applicable
NASA	National Aeronautics and Space Administration
n/d	nondimensional
NIST	National Institute for Standards and Technology
Pa	pascal
PDR	Preliminary Design Review
POAT	predicted operating/acceptance temperature
psf	pound per square foot
psi	pound per square inch
psia	pound per square inch absolute
QT	qualification temperature
s	second
scfm	cubic foot per minute at standard conditions
scms	cubic meter per second at standard conditions
SI	International System of Units
SM	standard manual
SPEC	specification

ST	survival temperature
STD	standard
TPSX	Thermal Protection Systems Expert
VJ	vacuum-jacketed
W	watt

This page was intentionally left blank.

ENGINEERING ANALYSIS, THERMAL/FLUID,

STANDARD FOR

1. SCOPE

This document defines the top-level requirements, methods, and boundary conditions that will be applied to all thermal and fluid analyses for systems designed and developed for use at John F. Kennedy Space Center (KSC), as well as for any spacecraft, instruments, and flight experiments designed and developed by KSC. This will include but is not limited to the following topics:

- required documentation,
- analysis guidelines,
- components,
- tubing and piping,
- heat transfer, and
- environments.

To ask questions or make suggestions about this standard or to request a variance to it, please refer to the Standardization Document Improvement Proposal at the end of the document.

2. APPLICABLE DOCUMENTS

Acceptable sources of thermophysical properties of fluids and materials are listed in Appendix A.

Additional sources cited by reference number throughout this standard are listed in Appendix B.

The following documents form a part of this document to the extent specified herein. When this document is used for procurement, including solicitations, or is added to an existing contract, the specific revision levels, amendments, and approval dates of said documents shall be specified in an attachment to the Solicitation/Statement of Work/Contract.

2.1 Governmental

Air Force Space Command

SMC-S-016	Test Requirements for Launch, Upper-Stage and Space Vehicles

Robert H. Goddard Space Flight Center (GSFC)

545-PG-8700.2.1A	Procedures and Guidelines: Requirements for Thermal Design, Analysis, and Development, NASA GSFC
GD-AP-2301	Earth Orbit Environmental Heating

John F. Kennedy Space Center (KSC)

KSC-SPEC-P-0027	Tubing, Superaustenitic Steel, Corrosion Resistant, UNS N08367 and UNS S31254, Seamed, Bright Annealed, Passivated, Specification for
KSC-SPEC-Z-0007	Tubing, Steel, Corrosion Resistant, Types 304 and 316, Seamless, Annealed, Specification for
KSC-SPEC-Z-0008	Fabrication and Installation of Flared Tube Assemblies and Installation of Fittings and Fitting Assemblies, Specification for
KSC-STD-Z-0005	Pneumatic Ground Support Equipment, Design of, Standard for
KSC-STD-Z-0008	Ground Life Support Systems and Equipment, Design of, Standard for
KSC-STD-Z-0009	Cryogenic Ground Support Equipment, Design of, Standard for

George C. Marshall Space Flight Center (MSFC)

MSFC-DWG-20M02540	Assessment of Flexible Lines for Flow Induced Vibration

National Aeronautics and Space Administration (NASA)

NASA-HDBK-1001	Terrestrial Environment (Climatic) Criteria Handbook for Use in Aerospace Vehicle Development
NASA-HDBK-8739.19-2	Measuring and Test Equipment Specifications, NASA Measurement Quality Assurance Handbook – Annex 2

(Copies of specifications, standards, drawings, and publications required by suppliers in connection with specified procurement functions shall be obtained from the procuring activity or as directed by the Contracting Officer.)

2.2 Non-Governmental

American National Standards Institute/International Society of Automation (ANSI/ISA)

ANSI/ISA 75.01.01	Flow Equations for Sizing Control Valves

American Society of Mechanical Engineers (ASME)

ASME B16.9	Factory-Made Wrought Buttwelding Fittings
ASME B31.3	Process Piping Guide
ASME B31.8	Gas Transmission and Distribution Piping Systems
ASME B36.10M	Welded and Seamless Wrought Steel Pipe
ASME B36.19M	Stainless Steel Pipe
ASME MFC-3M	Measurement of Fluid Flow in Pipes Using Orifice, Nozzle, and Venturi
ASME Section VIII, Division 1	Rules for Construction of Pressure Vessels
ASME V&V 20	Standard for Verification and Validation in Computational Fluid Dynamics and Heat Transfer

American Society for Testing and Materials (ASTM)

ASTM B88	Standard Specification for Seamless Copper Water Tube
ASTM MNL 36	Safe Use of Oxygen and Oxygen Systems: Handbook for Design, Operation, and Maintenance

3. NOMENCLATURE AND DEFINITIONS

A	area (mm^2) [in^2]
A_T	orifice throat area (m^2) [ft^2]
A_W	wall area (m^2) [ft^2]
a	thermal diffusivity (m^2/s) [ft^2/s]
C_d	orifice and nozzle discharge coefficient (n/d)
C_{sf}	surface-fluid constant

C_v	valve flow coefficient (n/d)
c_L	specific heat of liquid (J/kg) [Btu/lb_m·°R]
D_{eff}	effective diameter (mm) [in]
D_h	hydraulic diameter (mm) [in]
d_{BL}	baseline diameter (mm) [in]
d_i	inner diameter (mm) [in]
d_1	orifice inner diameter (mm) [in]
d_2	pipe inner diameter for orifice calculations (mm) [in]
f	friction factor (n/d)
f_t	friction factor (fully turbulent flow)
g	standard gravitational acceleration (9.807 m/s^2) [32.174 ft/s^2]
g_c	gravitational proportionality constant (1 kg·m/N·s^2) [32.174 lb_m·ft/lb_f·s^2]
H_L	head loss (m) [ft]
h_b	boiling coefficient (W/m^2·°C) [Btu/(hr·ft^2·°R)]
i_{fg}	heat of vaporization (J/kg) [Btu/lb_m]
J_a	Jakob number (n/d)
K	loss coefficient (n/d)
K_P	dimensionless quantity (n/d)
K_n	loss coefficient for pipe bends other than 90° (n/d)
K_1	upstream loss coefficient (n/d)
K_2	downstream loss coefficient (n/d)
$\mathrm{K}_{45°}$	loss coefficient for 45° bend or elbow (n/d)
$K_{90°}$	loss coefficient for 90° bend or elbow (n/d)
k	isentropic exponent (n/d)
k_L	thermal conductivity of liquid (W/m-°C)
L	length (mm) [in]
$\dot{m}$	mass flow rate (kg/s) [lb_m/s]
$n_{90°}$	number of 90° bends
P	pressure (Pa) [psia]
P_c	critical pressure (Pa) [psia]
P_R	rated pressure (Pa) [psia]

Pr_L	Prandtl number of liquid (n/d)
P_S	saturation pressure (Pa) [psia]
P_{SAT}	fluid saturation pressure (Pa) [psia]
P_{STD}	standard fluid pressure (Pa) [psia]
P_1	inlet pressure (Pa) [psia]
P_2	outlet pressure (Pa) [psia]
Q	heat transfer rate (W) [Btu/hr]
Q_R	rated volumetric flow rate (scms) [scfm]
Q_{STD}	volumetric flow rate at standard conditions (scms) [scfm]
q	boiling heat flux
R	constant of specific gas (N·m/kg·K) [$\mathrm{ft \cdot lb_f / lb_m \cdot °R}$]
R_e	Reynolds number (n/d)
$R_{e_{eff}}$	Reynolds number based on effective correction (n/d)
$R_{e_{D_h}}$	Reynolds number based on hydraulic diameter (n/d)
r	radius (mm) [in]
r	latent heat of vapor
r_a	inside radius of outer pipe for concentric pipes (mm) [in]
r_b	outside radius of inner pipe for concentric pipes (mm) [in]
T_R	rated fluid temperature (K) [°R]
T_{SAT}	fluid saturation temperature (K) [°R]
T_{STD}	standard fluid temperature (K) [°R]
T_W	wall temperature (K) [°R]
T_1	inlet temperature (K) [°R]
v	flow velocity (m/s) [ft/s]
X_t	pressure differential ratio (n/d)
Y	net expansion factor for compressible flows (n/d)
Z	compressibility factor (n/d)
Z_R	compressibility factor at rated conditions (n/d)
Z_{STD}	standard gas compressibility factor (n/d)
Z_1	compressibility factor at inlet conditions (n/d)
α	absorptivity (n/d)

β	diameter ratio (d_1/d_2) for orifice, nozzles, and venturi (n/d)
γ	gas-specific heat ratio (n/d)
γ''	specific weight of vapor (N/m^3) [lb$_f$/ft^3]
ΔPr	rated pressure drop (Pa) [psi]
ΔP	pressure differential (Pa) [psi]
ΔT	temperature differential
ε	emissivity (n/d)
ζ	correction factor for D_h
θ	angle of convergence or divergence in enlargements or contractions in pipes
λ	thermal conductivity of liquid (W/m·°C)
μ_L	viscosity of liquid (Pa·s) [lb$_m$/ft·hr]
ρ	density (kg/m^3) [lb$_m$/ft^3]
ρ_G	density of vapor (kg/m^3) [lb$_m$/ft^3]
ρ_L	density of liquid (kg/m^3) [lb$_m$/ft^3]
ρ_R	density at a rated condition (kg/m^3) [lb$_m$/ft^3]
ρ_{STD}	density at a standard condition (kg/m^3) [lb$_m$/ft^3]
σ	surface tension (N/m) [lb$_f$/ft]
σ_L	surface tension of liquid (N/m) [lb$_f$/ft]
υ	kinematic viscosity (m^2/s) [ft^2/s]
υ/a	Prandtl number of liquid (n/d)
φ	relative humidity (n/d)
ϵ	absolute roughness (mm) [in]

4. DOCUMENTATION AND SOFTWARE PACKAGES FOR THERMAL AND FLUID ANALYSIS

This section outlines the requirements for thermal and fluid analysis software packages. The selection of software to be used for a particular project or program shall be coordinated with the lead analyst and is typically defined in the analysis plan.

4.1 Incompressible Single-Phase Flow Analysis

A number of software packages are available to analyze fluid networks for which incompressible liquid flow (e.g., water or petroleum product flows) can be assumed. Many of these software packages are capable of only steady-state, single-phase flow analysis and are inappropriate for the analysis of cryogenic liquid flows because these cryogenic flows are frequently operated in near-saturation conditions. An example of a software package appropriate for analysis of incompressible single-phase flows is AFT Fathom.

4.2 Gaseous Flow Analysis

A number of software packages are available to analyze fluid networks (e.g., pneumatic systems, environmental control systems, and purges) operating in the gas phase. Though in many cases the ideal gas assumption is appropriate, the high range of operating pressures for KSC systems requires the use of software packages that can account for gas compressibility.

Many of these software packages are capable of only steady-state, single-phase flow analysis and are inappropriate for the analysis of the flow of gases at cryogenic temperatures. An example of a software package appropriate for analysis of noncryogenic gaseous flows is AFT Arrow.

4.3 Water Hammer Analysis

The analysis of fluid line pressure surge, or water hammer, is frequently required. Because water hammer is a transient phenomenon, appropriate surge analysis software is required. An example of a software package appropriate specifically for water hammer analysis is AFT Impulse. General-purpose flow network analysis software with full transient capability, such as SINDA/FLUINT, is also appropriate.

4.4 Saturated Flow Analysis

Systems operated at or near saturation conditions, commonly including cryogenic fluid systems, must be analyzed with software capable of multiphase flow calculations in order to accurately capture the behavior of the system. An example of a software package appropriate for analysis of systems operated at or near saturation conditions is SINDA/FLUINT.

4.5 Thermal Analysis

Thermal analysis of particular system components can often be performed in conjunction with the analyses described in 4.1 through 4.4. However, situations may arise where three-dimensional thermal analysis may be necessary. A variety of appropriate computer-aided design (CAD)-based analysis packages are available. An example of a software package appropriate for such analysis is Thermal Desktop.

5. SOLUTION INDEPENDENCE AND SENSITIVITY

5.1 Independent Solutions

All models shall be verified to have produced solutions that are independent of the time step or the number of elements used to make the fluid or thermal analysis model. If adjusting these parameters alters the results, the solution is not independent and is therefore inherently invalid.

5.1.1 Time Step Independence

Time steps for transient solutions shall be decreased or increased to verify that the solution achieved in the computational model is independent of the time step. Only results that have been verified to be independent of the time step are considered valid. A time step independent solution will have no greater than a 1.0% change in any of following: the time to steady state, temperature, pressure, or flow rate of the system being evaluated.

5.1.2 Fluid Node Independence

Fluid nodes used in computational models shall be tested for independent solutions. The number of nodes used to represent a fluid system shall be decreased or increased to verify that the solution achieved in the computational model is independent of the number of nodes used. Only results that have been verified to be independent of the number of fluid nodes are considered valid. A fluid node independent solution will have no greater than a 1.0% change in any of the following: the time to steady state, temperature, pressure, or flow rate of the system being evaluated.

5.1.3 Thermal Node Independence

Thermal nodes used in computational models shall be tested for independent solutions. The number of nodes used to represent thermal effects shall be decreased or increased to verify that the solution achieved in the computational model is independent of the number of nodes used. Only results that have been verified to be independent of the number of thermal nodes used are considered valid. A thermal node independent solution will have no greater than a 1.0% change in any of the following: the time to steady state, temperature, pressure, or flow rate of the system being evaluated.

5.1.4 Radiation Ray Independence

Radiation rays used in computational models shall be tested for independent solutions. The number of rays used shall be decreased or increased to verify that the solution achieved in the computational model is independent of the number of rays used. Only results that have been verified to be independent of the number of rays used are considered valid. A radiation ray independent solution will have no greater than a 1.0% change in temperature of the system being evaluated.

5.1.5 Mesh Independence

The size of elements in a computational fluid dynamics (CFD) mesh shall be tested for independent solutions. The number and size of elements shall be decreased or increased to verify that the solution achieved in the computational model is independent of the grid or mesh being used. Only results that have been verified to be independent of the grid or mesh used are considered independent.

5.2 Sensitivity Analysis

A sensitivity analysis shall be performed on a model to determine how the input parameters affect the output of the computational-model. Different types of sensitivity are described in more detail in NASA-HDBK-8739.19-2.

5.2.1 Single-Parameter Sensitivity Analysis

In single-parameter sensitivity analysis, the input parameters are assumed to be independent of one another, and only a single input parameter is changed at a time. The input values that shall be used for each test case are displayed as dots on cubes and are discussed in 5.2.1.1.

5.2.1.1 Two-Level Factorial Sensitivity Analysis

The two-level factorial method can be applied quickly and easily to early computer models. However, its applicability is limited because it can only show linear relationships between input and response values. For this method, three input factors (e.g., X_1, X_2, and X_3) may be varied, each having a maximum and minimum value, which would require a total of $2^3 = 8$ test cases. If these three factors were depicted in a three-dimensional plot, they would form a cube, as shown in Figure 1.

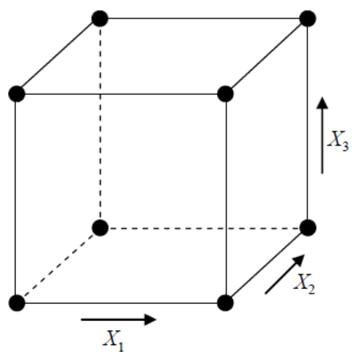

From NASA-HDBK-8739.19-2.

Figure 1. Two-Level 2^3 Factorial Input Parameter Cube

5.2.1.2 Three-Level Factorial Sensitivity Analysis

The three-level factorial method uses three input factors (e.g., X_1, X_2, and X_3) that may be varied. Each input factor has a maximum, minimum, and nominal value. This method can produce quadratic curves but requires a total of $3^3 = 27$ test cases to complete. If these three factors were depicted in a three-dimensional plot, they would form a cube, as shown in Figure 2. This figure excludes the point at the center of each face and the point at the center of the box, but these seven additional points shall be incorporated into the analysis.

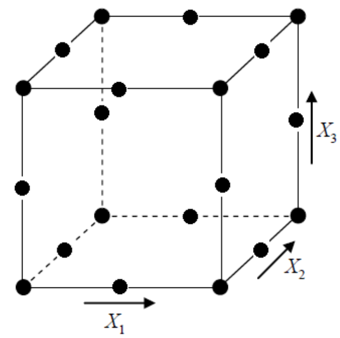

From NASA-HDBK-8739.19-2.

Figure 2. Three-Level 3^3 Factorial Input Parameter Cube

5.2.1.3 Box-Behnken Sensitivity Analysis

The Box-Behnken method uses three input factors (e.g., X_1, X_2, and X_3) that may be varied. Each input factor has a maximum, minimum, and nominal value. This method is a simpler version of the three-level factorial method and requires a total of 15 test cases to complete. If these three factors were depicted in a three-dimensional plot, they would form a cube, as shown in Figure 3.

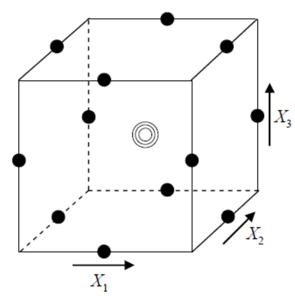

From NASA-HDBK-8739.19-2.

Figure 3. Box-Behnken Input Parameter Cube

5.2.2 Multiple-Parameter Sensitivity Analysis

In multiple-parameter sensitivity analysis, all input parameters are assigned a probability distribution, or uncertainty, that is propagated throughout the model, using a Monte Carlo simulation. This type of method accounts for input parameter interactions. This type of sensitivity analysis can be time-consuming and shall be completed as part of a Preliminary Design Review (PDR) deliverable.

5.3 Grid Converge Index (GCI)

GCI shall be performed in accordance with Section 2 of ASME V&V 20 in order to test for the convergence of structured and unstructured CFD grids and meshes.

5.3.1 Safety Factor for Structured Mesh

When GCI is used, a safety factor of 1.25 shall be applied to all structured mesh in accordance with Section 2 of ASME V&V 20.

5.3.2 Safety Factor for Unstructured Mesh

When GCI is used, a safety factor of 3.0 shall be applied to all unstructured mesh in accordance with Section 2 of ASME V&V 20.

5.4 Sensitivity Coefficients and Importance Factors

Sensitivity coefficients for input parameters to any computational model shall be determined using the methods outlined in Section 3 of ASME V&V 20.

Importance factors shall be used to determine which parameters will have the greatest effect on the solution of a computational model. These factors shall be determined using the methods outlined in Appendix B of ASME V&V 20.

5.5 Errors and Uncertainties

Errors and uncertainties between numerical simulations and experimental values shall be determined using the methods outlined in Section 1 of ASME V&V 20.

6. BOUNDING CONDITIONS AND DESIGN MARGINS

6.1 Bounding Cases

Thermal and fluid systems need to be evaluated to ensure that they will meet the requirements for the project under the worst-case thermal and fluid conditions that can be expected for the system.

6.1.1 Ground System Thermal Bounding Conditions

The worst-case parameters for ground system thermal analysis are outlined in Table 1.

Table 1. Worst-Case Parameters for Ground Thermal Analysis

Hot Operating Condition	Cold Operating Condition
Max environmental fluxes (diffuse and direct)	Min environmental fluxes (diffuse and direct)
Max indoor/outdoor ambient temperature	Min indoor/outdoor ambient temperature
Interface conductance that will produce the hottest temperatures	Interface conduction that will produce the coldest temperatures
Max α/Min ε of thermal coatings (degraded values)	Min α, Max ε of thermal coatings
Min blanket ε^* if the heat flow is out, Max if heat flow is in	Max blanket ε^* if the heat flow is out, Min if heat flow is in
Forced convection for insulation Natural convection for vaporization	Forced convection for insulation Natural convection for vaporization
Min frost accumulation on surface for insulation, Max for vaporization	Min frost accumulation on surface for insulation, Max for vaporization
Max ice accumulation on surface for insulation, Min for vaporization	Max ice accumulation on surface for insulation, Min for vaporization
α = absorptivity ε = emissivity ε^* = effective emissivity	

6.1.2 Spacecraft Thermal Bounding Conditions

The worst-case parameters for spacecraft thermal analysis are discussed in 545-PG-8700.2.1A and are outlined in Table 2.

Table 2. Worst-Case Parameters for Spacecraft Thermal Analysis

Hot Operating Condition	Cold Operating Condition	Hot Survival Condition	Cold Survival Condition
Max environmental incident fluxes (solar, albedo, IR) for science data collecting orbit	Min environmental incident fluxes (solar, albedo, IR) for science data collecting orbit	Max environmental incident fluxes (solar, albedo, IR) during mission	Min environmental incident fluxes (solar, albedo, IR) during mission
Max α/Min ε of thermal coatings (degraded values)	Min α, Max ε of thermal coatings (ideal values)	Max α, Min ε of thermal coatings (degraded values)	Min α, Max ε of thermal coatings (ideal values)
Max orbital average and/ or power dissipation	Min orbital average and/or transient power dissipation	Biased high heater set points and/or transient power dissipation	Biased low heater set points and/or transient power dissipation
Interface conduction that produces the hottest temperatures	Interface conduction that produces the coldest temperatures	Interface conduction that produces the hottest temperatures	Interface conduction that produces the coldest temperatures
Min blanket ε^* if the heat flow is out, Max if heat flow is in	Max blanket ε^* if the heat flow is out, Min if heat flow is in	Min blanket ε^* if the heat flow is out, Max if heat flow is in	Max blanket ε^* if the heat flow is out, Min if heat flow is in
Min solar cell efficiency, Max α (for max solar cell temperature)	Max solar cell efficiency, Min α (for max solar cell temperature)	Min solar cell efficiency, Max α (for max solar cell temperature)	Max solar cell efficiency, Min α (for max solar cell temperature)
Max operational bus voltage (heater dissipation)	Min operational bus voltage (heater dissipation)	Max bus voltage (heater dissipation)	Min bus voltage (heater dissipation)
α = absorptivity ε = emissivity ε^* = effective emissivity			
From 545-PG-8700.2.1A.			

6.1.3 Fluid System Bounding Conditions

Fluid densities, particularly for gases and cryogenic liquids, are highly variable. Therefore, fluid systems shall be evaluated at the highest possible input pressure and the lowest possible input temperature, as well as the opposite case.

6.1.3.1 Backpressure in Vent Systems

Vent systems shall be sized to provide minimum backpressure, consistent with required venting flow rates. In no case shall the backpressure interfere with the proper operation of safety relief devices or pneumatically operated devices. A design analysis shall be performed to ensure that excessive backpressure will not occur in vent systems, as specified in KSC-STD-Z-0005 and ASME Section VIII, Division 1, Paragraph UG-135(g).

6.1.3.2 Gaseous Oxygen Velocity

The velocity of gaseous oxygen during normal flow conditions shall be kept under Mach 0.2, as specified in KSC-STD-Z-0005, or (30.48 meters per second (m/s) (100 feet per second [ft/s]), as specified in ASTM MNL 36. The reference that produces the most conservative value shall be used.

6.1.3.3 Gaseous Oxygen Pressure

The pressure difference across a filter or other component shall not be allowed to exceed 3%. Pressure differences greater than 3% absolute can ignite particles in oxygen-enriched systems (1).

6.1.4 Contingency Scenarios

Operational criteria may require that operational contingency scenarios be evaluated.

6.2 Flow Device Constraints and Considerations

This section outlines certain constraints that shall be addressed during analysis of a compressible fluid system, as well as any considerations that shall be addressed in the analysis. In this section, *shall* denotes a constraint on the system, and *should* denotes a consideration or recommendation for the system.

6.2.1 Flexible Metal Hoses

Flow-induced vibration shall be addressed in any design that uses convoluted, unlined bellows or flexible metal hoses, as specified in MSFC-DWG-20M-02540.

6.2.2 Pressure Relief Devices

The relieving capability of the relief device shall be equal to or greater than the maximum flow capability of the upstream pressure regulator or pressure source and shall prevent the pressure from rising more than 10% above the system design pressure, as specified in KSC-STD-Z-0005; ASME B31.3, Paragraphs 301.2 and 322.6.3; and ASME Section VIII, Division 1; and ASME B31.8, Section 845. Pressure relief devices for cryogenic systems shall also reseat at greater than 85% of their set pressure, as specified in KSC-STD-Z-0009.

6.2.3 Fusible Plug/Burst Disk

A fusible plug or burst disk assembly shall comply with the following requirements, as specified in KSC-STD-Z-0008.

- The burst disk shall burst at the pressure vessel's maximum allowable working pressure plus 10% to 30%.

- The discharge flow rate, upon rupture of the burst disc, shall not be less than the flow rate of the nearest downstream relief valve.

6.2.4 Regulators

In pressure regulators, the ratio of the upstream pressure to the downstream pressure shall not exceed 5, as specified in KSC-STD-Z-0005 for compressible gas systems. This practice increases control of the pressure and flow and reduces problems in sizing a pressure-relieving device. The pressure regulator shall comply with the following additional requirements as specified in KSC-STD-Z-0008 for ground life support systems:

- The pressure reduction (outlet) shall not be less than 2% of the supply pressure (inlet) for a one-stage regulator.

- The accuracy of the pressure regulator shall be within 10% of its specified setting throughout the specified pressure supply (inlet) range.

6.2.4.1 Pressure-Regulating Circuits

The design of pressure-regulating circuits shall be predicated upon a detailed analysis of the system requirements, including those downstream of the design interface. This analysis shall consider but shall not be limited to the following items, as specified in KSC-STD-Z-0005:

- required accuracy of regulation,

- minimum and maximum flow rates expected,

- reliability required, and

- operational requirements.

6.2.4.2 Flow Rate Contingency Factor

Pressure-regulating circuits shall be designed to maintain the outlet pressure within required tolerances at a flow rate not less than 20% above the normal system requirements, as specified in KSC-STD-Z-0005.

6.2.4.3 Regulator Flow Scenarios

Regulators used in pneumatic systems shall be evaluated under two different flow scenarios: nominal conditions and low-density conditions. A regulator shall not be used if it cannot deliver the required flow under both of these conditions.

6.2.4.3.1 Nominal Conditions

Run the model, using the nominal expected pressure and temperature as inlet conditions. Verify that the pressure drop and flow through the system are within acceptable limits.

6.2.4.3.2 Low-Density Conditions

Run the model, using the lowest expected pressure and highest expected temperature as inlet conditions. Verify that the pressure drop and flow through the system under low-density conditions are within acceptable limits.

6.2.4.4 Regulator Failure/Relief Valve Scenarios

For each regulator and relief valve combination, separate failure scenarios shall be run. Run the following four conditions to verify that the flow rate is within the rated capability of the relief valve and that the tubing or piping between the regulator and relief valve is large enough to prevent overpressurization of the system. The stagnation pressure immediately downstream of each regulator shall not exceed 110% of the set pressure for the corresponding relief valve in any of the conditions described in 6.2.4.4.1 and 6.2.4.4.2.

6.2.4.4.1 All-Upstream-Losses Condition

Set the regulator to fail in the “Fully Open–No Control” position, and close the tubing downstream of the relief valve tee. This will force all flow to travel through the relief valve.

6.2.4.4.2 No-Upstream-Losses Condition

Set all loss coefficient values in components upstream of the regulator to “zero.” Also set all tubing or piping upstream of the regulator to “frictionless.”

6.3 Design Margins

Design margins shall be used in the thermal analysis of a system in order to help the system achieve at least a 95% confidence level. A summary sheet of all thermal/fluid design margins is incorporated in Appendix C.

6.3.1 Design Margins for Fluid Flow

Design margins shall be applied to the flow rates of all fluid flow systems. These margins shall be the same for the design and the analysis of ground support equipment and spacecraft systems.

6.3.1.1 Design Margins for Compressible-Gas Flow

Design margins shall be applied to the flow rates of all compressible-gas systems. These margins shall be applied to the nominal flow required for the system and shall not be smaller than the margins outlined in this section. Design margins shall vary depending on the maturity of the design, as outlined in Appendix C.

According to KSC-STD-Z-0005 and 6.2.4.2, a flow margin of ±20% shall be used on nominal desired flow of the system to determine high-flow and low-flow conditions. A safety factor of 2.5 was applied to this value to obtain the maximum design margin to be used during design and analysis. The safety factor was established by the chief engineer, and deviation requires the chief engineer’s approval.

6.3.1.2 Design Margins for Incompressible-Liquid Flow

Design margins shall be applied to the flow rates of all incompressible-liquid or cryogenic systems. These margins shall be applied to the nominal flow required for the system and shall not be smaller than the margins outlined in this section. Design margins shall vary depending on the maturity of the design, as outlined in Appendix C.

Historical data on pumped cryogenic systems has shown that flow rates may vary by ±25%. A safety factor of 2.0 was applied to this value to obtain the maximum design margin to be used during design and analysis. The safety factor applied was determined by the chief engineer.

6.3.2 Design Margins for Two-Phase Fluid Quality

Design margins shall be applied to the flow rates of all fluid systems where two-phase fluid quality is a concern, such as cryogenic systems. These margins shall be the same for the design and the analysis of ground support equipment and spacecraft systems. When maximum quality is required by the system, the quality margin that most constrains the system design shall be applied to that requirement. If the maximum quality allowed in a system is 0.0, then a margin shall be applied to the fluid temperature to keep the liquid in a subcooled state. Design margins shall vary depending on the maturity of the design, as outlined in Appendix C.

6.3.3 Thermal Design Margins for Ground Systems

Design margins shall be applied to the design and analysis of all ground systems. The correct margins to apply shall be whichever margins challenge the design the most. Design margins applied to the heat load of the system shall be evaluated first, since they are a higher-order boundary condition that shall challenge the system the most. For example, a system susceptible only to vacuum shall be evaluated by using radiation heat load design margins, whereas a heat exchanger or condenser shall be evaluated by using convection heat load design margins. Design margins shall vary depending on the maturity of the design, as outlined in Appendix C.

6.3.4 Thermal Design Margins for Spacecraft

Design margins shall be applied to all spacecraft projects and will vary depending on whether the system is passive or active. Passive systems shall apply design margins to temperatures, whereas active systems shall apply design margins to heat loads. Depending on the project or program, thermal design margins outlined in 545-PG-8700.2.1A or SMC-S-016 may be required and shall take precedence over the design margins outlined in this section.

a. A passive thermal control device or system is defined as having any of the following characteristics as outlined in (2):

    (1) constant-conductance or diode heat pipes,

    (2) hard-wired heaters (either fixed-resistance or variable-resistance, such as autotrace or positive-temperature-coefficient thermistors),

    (3) thermal storage devices (phase-change or sensible-heat),

    (4) thermal insulation (multilayer insulation [MLI], foams, or discrete shields),

    (5) radiators (fixed, articulated, or deployable) with louvers, or

    (6) surface finishes (coatings, paints, treatments, second-surface mirrors).

b. An active thermal control device or system is defined as having any of the following characteristics as outlined in (2):

    (1) variable-conductance heat pipes,

    (2) heat pumps and refrigerators,

    (3) stored-coolant subsystems,

    (4) heaters with commandable, mechanical, or electronic controllers,

    (5) capillary pumped loops,

(6) pumped fluid loops, or

(7) thermoelectric coolers.

6.3.4.1 Thermal Design Margins for Passive Systems

This section discusses the design margins that shall be used in the design and analysis of passive systems for spacecraft. The design margins outlined in Table 3 shall be assigned to temperature values. In addition, a 15% margin shall be applied to any project-approved power dissipation values.

Table 3. Thermal Margins for Passive Systems

		Concept	**Postacceptance Test**	**Mandatory Minimum**
Predicted Temperature (K/°R)		Thermal Uncertainty Margin (K)		
>203 K	(365.4 °R)	17	11	5
186–203 K	(334.8–365.4 °R)	16	10	5
168–185 K	(302.4–333.0 °R)	15	9	5
150–167 K	(270.0–300.6 °R)	14	8	5
132–149 K	(237.6–268.2 °R)	13	7	5
114–131 K	(205.2–235.8 °R)	11	6	5
96–113 K	(172.8–203.4 °R)	9	5	5
78–95 K	(140.4–171.0 °R)	8	4	4
60–77 K	(108.0–138.6 °R)	6	3	3
42–59 K	(75.6–106.2 °R)	4	2	2
23–41 K	(21.6–73.8 °R)	2	1	1
<23 K	(<21.6 °R)	1	1	1
From (2).				

6.3.4.2 Thermal Design Margins for Active Systems

This section discusses the design margins that shall be used in the design and analysis of active systems for spacecraft. Limits and margins that shall be assigned to heat load values are outlined in Table 4. In addition, a 15% margin shall be applied to any project-approved power dissipation values. For actively controlled systems (e.g., pumped fluid loops), a heat load margin, shown in Table 4, shall be used as specified in (2), in lieu of the minimum expected temperature.

Table 4. Thermal Margins for Active Systems

	Concept	**Preliminary Design Review (PDR)**	**Critical Design Review (CDR)**	**Qualification**	**Acceptance**
Heat Load Margin	50%	45%	35%	30%	25%

Heaters shall be sized using one of the following criteria as specified in 545-PG-8700.2.1A.

a. The hardware does not drop below temperature limits if the heater is at the minimum voltage and at 70% duty cycle (30% margin) under worst-case environmental conditions. The heater control point shall be set slightly above the allowable temperatures.

b. The heater shall be fully saturated (100% duty cycle or 0% margin) if the control point of the heater is more than 10 degrees Celsius (°C) (18 degrees Fahrenheit [°F]) above the allowable temperature.

7. COMPONENT INPUTS

This section discusses the methods for determining the relevant flow characteristics of components to be used in the analyzed system, including components in KSC control drawings or vendor control drawings. All component characteristics shall be represented by calculating the loss coefficient at the component's rated condition for its rated fluid commodity, unless otherwise specified for an individual component type.

7.1 Standard Conditions

Standard conditions in the English system are assumed to be P_{STD} = 14.7 pounds per square inch absolute (psia) and T_{STD} = 519.67 °R (101.325 kilopascals [kPa] and 15 °C).

7.2 Component Documentation

The manufacturer, model, and part numbers for all components shall be identified in the analysis documentation. All components shall be modeled using KSC specification or vendor drawing data, when available. All components shall be modeled using the resistance coefficient K for that component at its rated conditions and working fluid.

7.3 Loss Coefficient

Use of the loss (or resistance) coefficient (K) is preferred for fluid network calculations. When only the flow coefficient (C_v) is available, Eq. 1 can be used to determine the loss coefficient for components. This equation determines the loss coefficient as a function of the flow coefficient and internal diameter in inches. This equation is valid for compressible and incompressible fluids that do not have high viscosity.

$$K = \frac{890.3 d_i^{\,4}}{C_v^{\,2}} \qquad \text{Eq. 1}$$

Derived from Equation 2-11 of (3), *page 2-9.*
Replace 890.3 with 0.002139 for equations that use the International System of Units (SI).

For straight piping and tubing, the loss coefficient can be determined by using the friction factors outlined in 7.4, along with Eq. 2. The turbulent friction factor may replace the laminar friction in Eq. 2 for turbulent flow conditions.

$$K = f \cdot \frac{L}{d_i} \qquad \text{Eq. 2}$$

From Equation 2-4 of (3), *page 2-7.*

7.4 Friction Factor

7.4.1 Friction Factor in Circular Pipes

In most cases, the approximate friction factor may be determined by the Moody diagram, found on pages A-24 through A-26 of (3). For more explicit results, the friction factor may be calculated. For laminar flow (R_e < 2000), the friction factor is found by Eq. 3.

$$f = \frac{64}{R_e} \qquad \text{Eq. 3}$$

From Equation 1-18 of (3), *page 1-6.*

Flow in the turbulent region (R_e > 4000) may be found by the Colebrook equation, Eq. 4:

$$\frac{1}{\sqrt{f}} = -2.0\log\left(\frac{\epsilon}{3.7d_i} + \frac{2.51}{R_e\sqrt{f}}\right) \qquad \text{Eq. 4}$$

From Equation 1-20 of (3), *page 1-7.*

Eq. 4 requires an iterative solution for *f*, which may be accomplished using programs such as Microsoft Excel or MathCAD. Alternatively, a form of the Colebrook equation applicable for fully turbulent flow (Eq. 5) or the approximations given on page 1-7 of (3) may be used.

$$f_t = \frac{0.25}{\left[\log\frac{\left(\frac{\epsilon}{d_i}\right)}{3.7}\right]^2} \qquad \text{Eq. 5}$$

From Equation 2-8 of (3), *page 2-9.*

7.4.2 Friction Factor in Concentric Cylinders With Concentric Annuluses

For flow through the annulus of two concentric cylinders, the friction factors are larger than standard flow through a circular pipe. For calculating the friction factor through the annulus, the hydraulic diameter is used in place of the actual diameter. The hydraulic diameter is found by Eq. 6.

$$D_h = 2 \cdot (r_a - r_b) \qquad \text{Eq. 6}$$

From Equation 6-75 of (4), *page 381.*

The dimensionless term, ζ, is a correction factor for the hydraulic diameter that can be found from Eq. 7.

$$\zeta = \frac{(r_a - r_b)^2 \cdot (r_a{}^2 - r_b{}^2)}{r_a{}^4 - r_b{}^4 - \dfrac{(r_a{}^2 - r_b{}^2)^2}{\ln\left(\dfrac{r_a}{r_b}\right)}} \qquad \text{Eq. 7}$$

From Equation 6-76 of (4), *page 381.*

The effective Reynolds number is needed to determine the friction factor and is found by Eq. 8. The Reynolds number based on the hydraulic diameter will need to be determined using the actual flow area to determine the average velocity.

$$R_{e_{eff}} = \frac{1}{\zeta} \cdot R_{e_{D_h}} \qquad \text{Eq. 8}$$

From Equation 6-77 of (4), *page 381.*

For a laminar flow, the friction factor in concentric annular flow is found by Eq. 9.

$$f = \frac{64}{R_{e_{eff}}} \qquad \text{Eq. 9}$$

From Equation 6-77 of (4), *page 381.*

For turbulent flow in a concentric annulus, the friction factor may be found by using the Colebrook equation, Eq. 4, with minor changes. The hydraulic Reynolds number shall be used in place of the Reynolds number. Also, the effective diameter replaces the regular diameter, which is found using Eq. 10.

$$D_{eff} = \frac{D_h}{\zeta} \qquad \text{Eq. 10}$$

From Equation 6-77 of (4), *page 381.*

The updated form of the Colebrook equation for concentric annular flow is shown in Eq. 11.

$$\frac{1}{\sqrt{f}} = -2.0\log\left(\frac{\frac{\epsilon}{D_{eff}}}{3.7} + \frac{2.51}{R_{e_{D_h}}\sqrt{f}}\right) \qquad \text{Eq. 11}$$

From Example 6.14 of (4)*, pages 381-382.*

Alternatively, an adjusted form of Eq. 5, using the effective diameter instead of the diameter, may be tried and compared with iterative results from Eq. 11.

7.5 Pressure Loss

The pressure loss may be determined easily once the loss coefficient and friction factors are determined. Applying these known values to Eq. 12 will calculate the loss of static pressure head, also known as head loss.

$$H_L = K \cdot \frac{v^2}{2 \cdot g} \qquad \text{Eq. 12}$$

From Equation 2-3 of (3)*, page 2-7.*

The head loss may then be applied to Eq. 13 to determine the differential pressure loss.

$$\Delta P = H_L \cdot \rho \cdot g \qquad \text{Eq. 13}$$

From Equation 11.2 of (4)*, page 751.*

If the head loss was not determined before the differential pressure drop was solved, then Eq. 14 may be used to calculate the differential pressure drop directly. The turbulent friction factor may be used in lieu of the laminar friction factor in Eq. 14 when applicable.

$$\Delta P = f \cdot \frac{L}{d_i} \cdot \frac{v^2}{2 \cdot g} \cdot \frac{\rho}{144} \qquad \text{Eq. 14}$$

From Equation 1-17 of (3)*, page 1-6.*
Replace 144 with 1 for SI units.

7.6 Components

In the majority of cases, analysis software will provide acceptable correlations (upon verification) for losses due to components. When hand calculations are performed or when software correlations are not available, the remaining sections apply.

7.6.1 Regulators and Valves

The loss coefficient for all valves, check valves, and regulators shall be determined from either KSC component specification drawings or vendor drawings whenever possible. Flow coefficients shall be converted to loss coefficients via Eq. 2.

When KSC component specifications or vendor drawings are not available for a particular valve, the methods outlined for flow without attached fittings in ANSI/ISA 75.01.01 shall be used to determine the flow coefficient, which will then be converted to loss coefficient for modeling use. The listed applicability check for each equation shall also be performed to determine if the use of that equation is acceptable and shall be noted in the analysis documentation. ANSI/ISA 75.01.01 contains equations applicable for both compressible and incompressible fluids.

When ANSI/ISA 75.01.01 is used to determine the flow coefficient of a valve that is to be used in compressible fluid service, a pressure differential ratio (X_t) shall be specified. A nominal value shall be selected from Table 2 of ANSI/ISA 75.01.01, based on the type of valve being used. In addition, a high and low value of 0.3 and 0.9 shall be used to determine the minimum and maximum range for determining whether a component is choking.

A spreadsheet shall be available supplying loss coefficients for both compressible and incompressible components.

7.6.2 Filters

The loss coefficient for filters shall be determined using Eq. 15, unless specifically supplied by vendors or drawings. A spreadsheet (5) is available on the Design and Analysis Wiki page (6) to assist NASA and contractor personnel with these calculations. Eq. 15 was derived from the Darcy equation from (3). The derivation is shown in Appendix D.

$$K = \left(\frac{60}{144}\right)^2 \cdot \frac{g \cdot \pi^2 \cdot R \cdot P_R \cdot \Delta P_R \cdot Z_{STD}{}^2 \cdot T_{STD}{}^2 \cdot d_{BL}{}^4}{8 \cdot P_{STD}{}^2 \cdot Q_R{}^2 \cdot Z \cdot T_R} \qquad \text{Eq. 15}$$

Derived by Stephen Van Genderen from equations in (3).
Replace $(60/144)^2$ *with* $(1/1000000)^2$ *for SI units.*

For incompressible flows, the loss coefficient value shall be determined via Eq. 2 and the calculation spreadsheet for incompressible fluids to be provided.

7.6.3 Orifices and Cavitating Flows

Orifice behavior for gases can be determined using the following equations.

$$\dot{m} = C_d A_T \rho \sqrt{2 g_c \frac{\gamma}{\gamma - 1} Z_1 R T_1 \left[\left(\frac{P_2}{P_1}\right)^{\frac{2}{\gamma}} - \left(\frac{P_2}{P_1}\right)^{\frac{\gamma+1}{\gamma}} \right]} \qquad \text{Eq. 16}$$

Equation 3.8.2.3b of (7).

$$\dot{m} = 144 \cdot C_d A_T P_1 \sqrt{\frac{g_c \gamma}{Z_1 R T_1} \left(\frac{2}{\gamma + 1}\right)^{\frac{\gamma+1}{\gamma-1}}} \qquad \text{Eq. 17}$$

Equation 3.8.2.3g of (7).
Remove the 144 for SI units.

Use Eq. 16 when $\frac{P_2}{P_1} > \frac{P_c}{P_1}$. Use Eq. 17 when $\frac{P_2}{P_1} < \frac{P_c}{P_1}$. Use Eq. 18 to determine the ratio of critical pressure to inlet pressure to be used in the above-mentioned conditions.

$$P_c = P_1\left(\frac{2}{\gamma+1}\right)^{\frac{\gamma}{\gamma-1}} \qquad \text{Eq. 18}$$

Equation 3.3.8.9d of (7).

For cavitated liquid flow (as in a cavitating venturi or liquid orifice), Eq. 19 shall be used.

$$\dot{m} = C_d A_T \sqrt{\frac{144 \cdot 2 g_c \rho \left(P_1 - P_s\right)}{\left(1-\beta^4\right)}} \qquad \text{Eq. 19}$$

From Equations 4-5 and 4-6 of (3).
Remove the 144 for SI units.

Common engineering practice has been to assume a C_d of 0.6 for orifices. More recent work has developed some empirical correlations for C_d for orifices, nozzles, and venturis. These are found in (1) as Equations 4-7 through 4-13. If C_d is known for an orifice plate or for an ISA 1932 or a long-radius nozzle, the loss coefficient may be found as follows:

$$K = \left[\frac{\sqrt{1-\beta^4 \cdot \left(1-C_d^2\right)}}{C_d \cdot \beta^2} - 1\right]^2 \qquad \text{Eq. 20}$$

From ASME MFC-3M, Equation 2-10, page 26.

A relationship between equivalent sharp-edged orifice diameter and flow coefficient is given by Eq. 21.

$$d_1 = 0.236\sqrt{C_v} \qquad \text{Eq. 21}$$

From (8).

A spreadsheet shall be available to determine loss coefficients for both compressible and incompressible orifices under choked and unchoked conditions. The discharge coefficient for subcritical, unchoked flows for both compressible and incompressible fluids is a function of the pipe Reynolds number. Since the Reynolds number changes based on the fluid flow rate, the equations to calculate the flow coefficient for an unchoked orifice shall be used only in hand calculations.

7.6.3.1 Discharge Coefficients for Orifice Plates

As stated in 7.6.3, the discharge coefficient for orifice plates has been determined to be a function of the Reynolds number from the upstream pipe. Further information on this relationship is discussed in ASME MFC-3M, which is summarized in (3). The relationships outlined in Eq. 22 through Eq. 24 are limited to use under the following conditions.

a. For orifice plates with corner or with D and ½ D pressure taps:

(1) $d_1 \geq 12.5$ mm (0.5 in)

(2) 50 mm (2 in) $\leq d_2 \leq$ 1000 mm (40 in)

(3) $0.10 \leq \beta \leq 0.75$

(4) $R_e \geq 5000$ for $0.10 \leq \beta \leq 0.56$

(5) $R_e \geq 16{,}000\beta^2$ for $\beta > 0.56$

b. For orifice plates with flange taps:

(1) $d_1 \geq 12.5$ mm (0.5 in)

(2) 50 mm (2 in) $\leq d_2 \leq$ 1000 mm (40 in)

(3) $0.10 \leq \beta \leq 0.75$

(4) $R_e \geq 5000$ and $R_e \geq 170\beta^2 d_2$ (d_2, millimeters) ($R_e \geq 4318\beta^2 d_2$ [d_2, inches])

c. For gases, $0.80 < (P_2/P_1) < 1.00$

d. $\triangle P \leq 250348.6$ Pa (36.31 pounds per square inch [psi])

The discharge coefficient for orifice plates is determined by Eq. 22. The ratio L_1 is the distance from the upstream tap to the upstream orifice plate face, divided by the pipe diameter. The ratio L_2 is the distance of the downstream tap from the downstream orifice plate face, divided by the pipe diameter.

$$C_d = 0.5961 + 0.0261\beta^2 - 0.216\beta^8 + 0.000521\cdot\left(\frac{10^6\cdot\beta}{R_e}\right)^{0.7}$$
$$+\left(0.0188 + 0.0063\cdot\left(\frac{19000\beta}{R_e}\right)^{0.8}\right)\cdot\beta^{3.5}\cdot\left(\frac{10^6}{R_e}\right)^{0.3}$$
$$+\left(0.043 + 0.080e^{-10L_1} - 0.123e^{-7L_1}\right)\cdot\left(1 - 0.11\cdot\left(\frac{19000\beta}{R_e}\right)^{0.8}\right)\cdot\frac{\beta^4}{1-\beta^4}$$
$$-0.031\cdot\left(\left(\frac{2L_2}{1-\beta}\right) - 0.8\cdot\left(\frac{2L_2}{1-\beta}\right)^{1.1}\right)\cdot\beta^{1.3}$$

From ASME MFC-3M, Equation 2-4, page 25. Eq. 22

Values for L_1 and L_2 to be used in Eq. 22 are as follows:

- Corner taps: $L_1 = L_2 = 0$
- D and ½ D pressure taps: $L_1 = 1$, $L_2 = 0.47$
- Flange taps: $L_1 = L_2 = 1/d_2$

If the inner diameter (d_2) of the pipe is less than 71.12 mm (2.8 in), the term shown as Eq. 23 shall be added onto Eq. 22.

$$+0.011\cdot(0.75-\beta)\cdot(2.8-d_2)$$ Eq. 23

From ASME MFC-3M, Equation 2-5, page 25.
Divide d_2 by 25.4 for SI units.

7.6.3.2 Expansion Factor for Orifice Plates

The expansibility factor for compressible flow through an orifice plate may be needed for some unchoked conditions and is determine by Eq. 24. The isentropic exponent may be replaced with the gas specific heat ratio for an ideal gas.

$$Y = 1 - \left(0.351 + 0.256\beta^4 + 0.93\beta^8\right)\cdot\left[1 - \left(\frac{P_2}{P_1}\right)^{\frac{1}{k}}\right]$$ Eq. 24

From ASME MFC-3M, Equation 2-6, page 25.

7.6.3.3 Discharge Coefficient for Flow Nozzles

The discharge coefficient for flow nozzles is dependent on the Reynolds number of the flow. Further information on this relationship is discussed in ASME MFC-3M, which is summarized in (2).

a. For ISA 1932 flow nozzles, the discharge coefficient is given by Eq. 25. For ISA 1932 flow nozzles, Eq. 25 is used only when the following conditions are satisfied.

(1) 50 mm (2 in) $\leq d_2 \leq$ 500 mm (2 in)

(2) $0.30 \leq \beta \leq 0.80$

(3) $7\ (10^4) \leq R_e \leq 1\ (10^7)$ for $0.30 \leq \beta \leq 0.44$

(4) $2\ (10^4) \leq R_e \leq 1\ (10^7)$ for $0.44 \leq \beta \leq 0.80$

$$C_d = 0.9900 - 0.2262\beta^{4.1} - \left(0.00175\beta^2 - 0.0033\beta^{4.15}\right)\cdot\left(\frac{10^6}{R_e}\right)^{1.15} \qquad \text{Eq. 25}$$

From ASME MFC-3M, Equation 3-6, page 52.

b. For long-radius flow nozzles, the discharge coefficient is given by Eq. 26 and must satisfy the following conditions to be acceptable for use.

(1) 50 mm (2 in) $\leq d_2 \leq$ 630 mm (25 in)

(2) $0.20 \leq \beta \leq 0.80$

(3) $1\ (10^4) \leq R_e \leq 1\ (10^7)$

(4) $\varepsilon/d_2 \leq 3.2\ (10^{-4})$

$$C_d = 0.9965 - 0.00653\beta^{0.5}\left(\frac{10^6}{R_e}\right)^{0.5} \qquad \text{Eq. 26}$$

From ASME MFC-3M, Equation 3-12, page 55.

c. For venturi nozzles, the discharge coefficient is given by Eq. 27 and must satisfy the following conditions to be acceptable for use.

(1) 65 mm (2.5 in) $\leq d_2 \leq$ 500 mm (20 in)

(2) $d_1 \geq$ 50 mm (2 in)

(3) $0.316 \leq \beta \leq 0.775$

(4) $1.5\ (10^5) \leq R_e \leq 2\ (10^6)$

$$C_d = 0.9858 - 0.196\beta^{4.5} \qquad \text{Eq. 27}$$

From ASME MFC-3M, Equation 3-16, page 57.

7.6.3.4 Discharge Coefficients for Venturi Meters

The discharge coefficient for venturi meters is dependent on the method of manufacturing. The values for these methods are listed here, but analysts are advised to cite the source of this information. See ASME MFC-3M, Sections 4-4.5.2, 3, and 4 (page 73), for more detailed information.

a. "As-Cast" convergent section: C_d = 0.984

(1) 100 mm (4 in) $\leq d_2 \leq$ 1200 mm (48 in)

(2) $0.30 \leq \beta \leq 0.75$

(3) $2\ (10^5) \leq R_e \leq 6\ (10^6)$

b. Machined convergent section: C_d = 0.995

(1) 50 mm (2 in) $\leq d_2 \leq$ 250 mm (10 in)

(2) $0.30 \leq \beta \leq 0.75$

(3) $2\ (10^5) \leq R_e \leq 6\ (10^6)$

c. Rough-welded convergent section: C_d = 0.985

(1) 100 mm (4 in) $\leq d_2 \leq$ 1200 mm (48 in)

(2) $0.30 \leq \beta \leq 0.75$

(3) $2\ (10^5) \leq R_e \leq 6\ (10^6)$

7.6.3.5 Expansion Factor for Flow Nozzles and Venturi Meters

The expansibility factor for compressible flow through a flow nozzle or venturi meter may be needed for some nonchoked conditions and is determined by Eq. 28. The isentropic exponent may be replaced with the gas specific heat ratio for an ideal gas.

$$Y = \left\{ \left(\frac{k \cdot \left(\frac{P_2}{P_1} \right)^{2/k}}{k-1} \right) \cdot \left(\frac{1-\beta^4}{1-\beta^4 \cdot \left(\frac{P_2}{P_1} \right)^{2/k}} \right) \cdot \left[\frac{1-\left(\frac{P_2}{P_1} \right)^{(k-1)/k}}{1-\left(\frac{P_2}{P_1} \right)} \right] \right\}^{0.5} \qquad \text{Eq. 28}$$

From ASME MFC-3M, Equation 4-3, page 73.

7.6.4 Relief Valves

Relief valves are pressure-relieving devices that have an internal orifice and shall be sized for the maximum flow rate possible through an orifice under choked flow conditions. The equations used to determine the flow rate through a relief valve are outlined in 7.6.3.

7.6.4.1 Relief Valve Sizing for Cryogenic Systems

Relief valve for cryogenic service shall be able to expel gas at a higher flow rate than can be vaporized inside a vacuum-jacketed (VJ) section. Sizing for cryogenic relief valves is a complicated process and shall be calculated using the following assumptions.

- The VJ section has no thermal resistance.
- The cryogenic fluid is saturated at the relief valve set pressure.
- The heat flux is composed of direct and diffuse solar radiation.
- The heat flux shall be for hottest day of the year.
- The worst-case temperature for the relief valve area is (70 °C) (158 °F).
- The outer VJ pipe shall have an absorptivity of 1.0.

A spreadsheet shall be available to size cryogenic system relief valves based on the maximum direct and diffuse solar radiation a VJ line will experience. Heat leak from connected cryogenic lines can be added to the total heat entering the VJ section.

7.6.4.2 Relief Valve Sizing for Pneumatic Systems

Relief valves for pneumatic service shall be able to expel gas at a higher flow rate than can be delivered by a failed, fully open, upstream regulator. A spreadsheet shall be available to size pneumatic system relief valves based on the failure of the upstream regulator. In addition, regulator failure scenarios shall be evaluated in modeling tools that are approved for pneumatic system analysis.

7.6.5 Pumps

7.6.5.1 Centrifugal Pumps

Centrifugal pumps are considered to be head-generating pumps used for large flows and are the more commonly used pumps. Centrifugal pumps shall have a performance curve of the pump's pressure change versus flow rate for the commodity being analyzed. The inlet and outlet diameters, pump speed, and mechanical and hydraulic efficiencies shall also be provided. The mechanical and hydraulic efficiencies may be represented by a single or total efficiency.

7.6.5.2 Positive-Displacement Pumps

Positive-displacement pumps are flow-generating pumps that displace a fixed amount of fluid per shaft revolution. Positive-displacement pumps shall have a performance curve of the pump's flow rate versus pressure change for the commodity being analyzed. The following shall also be provided: inlet and outlet diameters; volumetric displacement per revolution; and volumetric, mechanic, and hydraulic efficiencies. The mechanical and hydraulic efficiencies may be represented by a single or total efficiency. The volumetric efficiency shall be provided as a separate value from both the mechanical and hydraulic efficiencies.

7.6.6 Flow-Induced Vibration

Flow-induced vibrations for flexible hoses shall be calculated in accordance with MSFC-DWG-20M02540.

7.6.7 Elbows and Bends

All flow losses from elbows and bends shall be accounted for in an analysis. Typically, all elbows in cryogenic systems are actual bends, not sudden changes in direction. Elbows shall be modeled as pipe bends unless otherwise directed.

The ratio of bend radius to inner diameter is determined by using ASME B16.9 for pipe bends or KSC-SPEC-Z-0008 for tubing bends. The loss coefficient for 90° bends is shown in Table 5. To determine the loss coefficient for bends other than 90°, use Eq. 29.

Table 5. Loss Coefficient for 90° Bends and Elbows

r/d	**1**	**1.5**	**2**	**3**	**4**	**6**
$K_{90°}$	$20f_t$	$14f_t$	$12f_t$	$12f_t$	$14f_t$	$17f_t$
r/d	**8**	**10**	**12**	**14**	**16**	**20**
$K_{90°}$	$24f_t$	$30f_t$	$34f_t$	$38f_t$	$42f_t$	$50f_t$
From the table in (3)*, page A-30.*						

$$K_n = \left(n_{90°} - 1\right) \cdot \left(0.25 \cdot \pi \cdot f_t \cdot \frac{r}{d} + 0.5 \cdot K_{90°}\right) + K_{90°} \qquad \text{Eq. 29}$$

From (3)*, page A-30.*

The loss coefficient is determined by Eq. 30 for a 90° elbow and Eq. 31 for a 45° elbow, substituting as appropriate.

$$K_{90°} = 30 \cdot f_t \qquad \text{Eq. 30}$$

From (3)*, for Standard Elbows, page A-30.*

$$K_{45°} = 16 \cdot f_t \qquad \text{Eq. 31}$$

From (3)*, for Standard Elbows, page A-30.*

7.6.7.1 Tees and Wyes

Recent work in the behavior of tees and wyes has shown them to be much more complicated than previously thought. For preliminary work, Figures 2-14 through 2-17 of (3) shall be used. More detailed analyses shall follow the procedure outlined beginning on page 2-14 of (3).

7.6.7.2 Area Changes

The loss coefficient through area changes in pipes or tubes are determined as follows:

Gradual contraction is defined as $\theta \leq 45°$ and shall be determined from Eq. 32.

$$K_1 = 0.8 \cdot \sin\frac{\theta}{2} \cdot \left(1 - \beta^2\right) \qquad \text{Eq. 32}$$

From Equation 2-26 of (3)*, page 2-11.*

Sudden contraction is defined as $45° < \theta \leq 180°$ and shall be determined from Eq. 33.

$$K_1 = 0.5 \cdot \sqrt{\sin\frac{\theta}{2}} \cdot \left(1 - \beta^2\right) \qquad \text{Eq. 33}$$

From Equation 2-27of (3)*, page 2-11.*

Gradual enlargement is defined as $\theta \leq 45°$ and shall be determined from Eq. 34.

$$K_1 = 2.6 \cdot \sin\frac{\theta}{2} \cdot \left(1-\beta^2\right)^2 \qquad \text{Eq. 34}$$

From Equation 2-24 of (3), *page 2-11.*

Sudden enlargement is defined as $45° < \theta \leq 180°$ and shall be determined from Eq. 35.

$$K_1 = \left(1-\beta^2\right)^2 \qquad \text{Eq. 35}$$

From Equation 2-25 of (3), *page 2-11.*

If the downstream loss coefficient is desired in place of the upstream loss coefficient, then it shall be determined by using Eq. 36.

$$K_2 = \frac{K_1}{\beta^4} \qquad \text{Eq. 36}$$

From Equation 2-19 of (3), *page 2-11.*

7.6.7.3 Additional Losses

Any losses not covered in this section shall be applied as a loss coefficient.

8. PIPING AND TUBING INPUTS

This section discusses the methods and inputs necessary to represent pressure and flow losses in an analyzed system. These methods shall be applied to both piping and tubing that will be analyzed in the system.

8.1 Piping and Tubing Roughness

The pipe roughness shall be taken into account during all calculations for a piping system. The absolute roughness values of commonly used materials are listed in Table 6.

Table 6. Absolute Roughness Values for Commonly Used Materials

Material (Source)	**Absolute Roughness mm (ft)**
AL6XN (KSC-SPEC-P-0027)	0.0008 (0.000003)
Stainless steel (4)	0.002 (0.000007)
Invar/iron (4)	0.046 (0.00015)
Brass/copper (4)	0.002 (0.000007)
Commercial steel	0.04572 (0.00015)

8.2 Piping and Tubing Wall Thickness

All outer diameters, inner diameters, and thicknesses of pipe walls shall be in accordance with the correct standards for that type of piping or tubing material, as listed in Table 7.

Table 7. Applicable Standards for Piping and Tubing Wall Thickness

Material	Applicable Standard
AL6XN	KSC-SPEC-P-0027
Stainless steel	ASME B36.19M
Invar/iron	ASME B36.10M
Steel	ASME B36.10M
Copper	ASTM B88
Stainless-steel tubing	KSC-SPEC-Z-0007E

8.3 Lengths

For friction losses to be accounted for accurately, the analysis shall include all pipe and tubing lengths. Meandering runs shall not be simplified.

8.4 Elevation

The effects of changes in elevation of piping or tubing runs on fluid and thermal properties shall be evaluated in order to provide the most accurate results.

9. HEAT TRANSFER

This section provides the methods and boundary conditions used to determine heat transfer calculations.

9.1 Material Properties

Temperature-dependent material properties outlined in Appendix A shall be used for all heat transfer calculations.

9.2 Fluid Properties

Fluid properties that cause variances in temperature or pressure, outlined in Appendix A, shall be used for all heat transfer calculations.

9.3 Optical Properties

9.3.1 Acceptable Sources of Optical Properties

Optical properties shall be obtained from test data whenever possible. Information for initial values is available from one of the following databases: Materials and Processes Technical Information System (MAPTIS), Thermal Protection System Expert (TPSX), or NESC Thermal Desktop Properties Database. Reference (9) is also a widely accepted source for optical properties of several materials and insulations.

9.3.2 Degradation of Optical Properties

When performance degradation of optical properties is a concern and no valid data is available, the absorptivity of the material can be increased 10% to15% to account for degradation. The emissivity of the material should not be altered. This increase should be used only during concept and should be replaced with material data as soon as it becomes available. GSFC should be contacted for material degradation information before using this increase.

9.4 Ground Environmental Conditions

Environmental conditions, such as the ambient temperatures, shall be those shown in NASA-HDBK-1001 or this document.

9.4.1 Ground Interior-Air Temperatures at KSC

The ambient interior temperatures used for heat transfer calculations shall be $T_{MAXIMUM}$ = 27 °C (80 °F) and $T_{MINIMUM}$ = 15 °C (60 °F).

Under extreme internal conditions for a maximum of 1 hour, the temperature values used shall be $T_{MAXIMUM}$ = 40 °C (104 °F) and $T_{MINIMUM}$ = 11 °C (52 °F).

9.4.2 Ground Exterior-Air Temperatures at KSC

The ambient exterior temperatures used for heat transfer calculations shall be $T_{MAXIMUM}$ = 38 °C (99 °F) and $T_{MINIMUM}$ = –6 °C (19 °F).

9.4.3 Ground Interior Relative Humidity at KSC

The interior relative humidity used for heat transfer calculations shall be $\varphi_{MINIMUM}$ = 30% and $\varphi_{MAXIMUM}$ = 70% at the temperatures specified in 9.4.1, with a nominal value of $\varphi_{NOMINAL}$ = 55%.

9.4.4 Ground Exterior Relative Humidity at KSC

The exterior relative humidity used for heat transfer calculations shall be $\varphi_{MINIMUM}$ = 5% and $\varphi_{MAXIMUM}$ = 100% at the temperatures specified in 9.4.2.

9.4.5 Ground Wind Velocities at KSC

The wind velocities outlined in Table 8 shall be used for heat transfer calculations.

Table 8. Ground Wind Profiles for Thermal Assessments

Height		1-Hour Steady-State Wind Speed Profile for Thermal Assessments			
		Design Low		Design High	
m	ft	m/s	ft/s	m/s	ft/s
10.0	33	0	0	11.8	38.71
18.3	60	0	0	13.5	44.29
30.5	100	0	0	15.2	49.87
61.0	200	0	0	17.8	58.40
91.4	300	0	0	19.5	63.98
121.9	400	0	0	20.8	68.24
152.4	500	0	0	21.9	71.85

9.4.6 Ground Solar Heating at KSC

The solar-flux values outlined in Table 9 shall be used for heat transfer calculations.

Table 9. Solar Flux as a Function of Time of Day

Local Time of Day	Design High Solar Radiation		Local Time of Day	Design Low Solar Radiation	
Hour	Btu/ft^2-hr	W/m^2	Hour	Btu/ft^2-hr	W/m^2
0500	0	0	0655	0	0.000
1100	363	1145	1100	70	220.821
1400	363	1145	1300	80	252.367
2000	0	0	1710	0	0.000

9.5 Space Environmental Conditions for Earth Orbit

Space environmental conditions, such as environmental heating, shall be taken from GD-AP-2301, which lists all boundary conditions for low Earth orbit and geosynchronous Earth orbit.

9.5.1 Deep-Space Temperature

For all Earth orbit analyses involving heat transfer, a deep-space temperature of 2.7 K (4.86 °R) shall be used.

9.5.2 Solar Constant

Solar-constant values for Earth orbit analyses shall be in accordance with GD-AP-2301. The solar-constant values used for heat transfer calculations are outlined in Table 10.

9.5.3 Albedo Factor

Albedo factor values for Earth orbit analyses shall be in accordance with GD-AP-2301. The albedo factor values used for heat transfer calculations are outlined in Table 10.

9.5.4 Earth-Emitted Energy

Values for Earth-emitted energy for Earth orbit analyses shall be in accordance with GD-AP-2301. Values for Earth-emitted energy used for heat transfer calculations are outlined in Table 10.

9.5.5 Equivalent Earth Temperatures

Equivalent Earth temperatures for Earth orbit analyses shall be in accordance with GD-AP-2301. The equivalent Earth temperatures used for heat transfer calculations are outlined in Table 10. The maximum and minimum values are normally used, except when seasonal information is needed for a project.

Table 10. Earth Solar and Albedo Ranges

Solar Constant (W/m^2)	Albedo Factor (n/d)	Earth-Emitted Energy (W/m^2)	Equiv. Earth Temp. (K)
Nominal 1368	0.25	256	258
	0.30	239	254
	0.35	222	250
Winter Solstice 1422	0.25	267	262
	0.30	249	258
	0.35	231	253
Summer Solstice 1318	0.25	247	256
	0.30	231	251
	0.35	214	246
From GD-AP-2301.			

9.6 Correlations

9.6.1 Empirical Correlations

Empirical correlations are very common in the study of heat transfer, particularly with respect to convection. The source of empirical correlations, as well as any applicable validity restrictions, shall be documented. Whenever possible, multiple correlation calculations shall be performed, with the most conservative valid result dominating.

9.6.2 Kutateladze Boiling Correlation Correction

When calculations for nucleate boiling are performed, the Kutateladze equation shall be used. This method as applied to cryogenic fluids is discussed in (10). A correction for this equation has been provided by Randall F. Barron and is attached in Appendix E. The three main equations used in this correlation are outlined below; however, Appendix E shall be consulted for the correct units and meanings of all variables.

The Jakob number (J_a) used is determined by using Eq. 37.

$$J_a = \frac{c_L \cdot (T_W - T_{SAT})}{i_{fg}} \qquad \text{Eq. 37}$$

From Equation 4-26 of (10), *page 164.*

The dimensionless parameter K_P is determined by using Eq. 38.

$$K_P = \frac{P_{SAT} \cdot 144}{\sqrt{(g / g_c) \cdot \sigma_L (\rho_L - \rho_G)}} \qquad \text{Eq. 38}$$

From Equation 4-25 of (10), *page 164.*
Remove the 144 for SI units.

Finally, the heat flux determined by the Kutateladze correlation is calculated by rearranging the derivation shown in Appendix E, which is displayed here as Eq. 39.

$$\frac{Q}{A_W} = \left(\frac{J_a \cdot 0.0007}{Pr_L^{0.65} \cdot \left(\frac{\rho_G}{\rho_L \cdot K_P} \right)^{0.7}} \right)^{10/3} \cdot \frac{\mu_L \cdot i_{fg}}{\sqrt{\frac{\sigma_L \cdot g_c}{g \cdot (\rho_L - \rho_G)}}} \qquad \text{Eq. 39}$$

From Equation 4-24 of (10), *page 164, and corrected in Appendix E.*

9.7 Frost and Ice Formation

When cryogenic systems with noninsulated lines are analyzed, the effects of frost or ice formation shall be taken into account. Simple methods of frost formation analysis are available in SINDA/FLUINT and from other sources. Since frost and ice can significantly affect the performance for a system, worst-case conditions, as defined in 6.1, shall be analyzed. Modeling frost effects with a constant heat rate or heat flux value is not recommended.

This page was intentionally left blank.

APPENDIX A. REFERENCES FOR THERMOPHYSICAL PROPERTIES OF FLUIDS AND MATERIALS

Fluid and material properties to be used in the analysis of fluid or thermal systems shall be in accordance with this document. Acceptable sources of material properties are the National Institute for Standards and Technology (NIST), the Thermal Protection Systems Expert (TPSX), MatWeb, and the Materials and Processes Technical Information System (MAPTIS). Acceptable sources of fluid properties are CRTech Property files, NIST's REFPROP database, and Chempak (AFT analysis only).

a. Fluid property references are listed here in the order of preference:

    (1) NIST REFPROP,

    (2) CRTech Fluid Property Files,

    (3) Chemical Equilibrium with Application (CEA),

    (4) CEA 2, and

    (5) Chempak (single-phase fluids only).

b. Material property references are listed here in the order of preference:

    (1) NIST Material Properties,

    (2) NESC Thermal Desktop Database (Optical and Thermophysical)

    (3) MAPTIS,

    (4) TPSX, and

    (5) MatWeb.

This page was intentionally left blank.

APPENDIX B. SPECIFIC REFERENCES

The following references contain supplemental information to guide the user in the application of this standard. References (1) through (11) are specifically cited in the body or in other appendices.

(1) Elliot Forsyth, *Fundamentals of Oxygen Systems Design & Analysis: Oxygen Safety Training Course Series,* Wendell Hull & Associates, Inc., 2010.

(2) Martin Donabedian, *Spacecraft Thermal Control Handbook,* Vol. 2: "Cryogenics," American Institute of Aeronautics and Astronautics, Inc., 2003.

(3) Crane Company, *Flow of Fluids Through Valve, Fittings and Pipe,* Technical Paper No. 410, Crane Company, Stamford, Connecticut, 2009.

(4) Frank M. White, *Fluid Mechanics,* 5th ed., McGraw-Hill, New York, 2003.

(5) Stephen Van Genderen, *Filter K Value Calculation Spreadsheet*, Kennedy Space Center, Florida.

(6) Stephen Anthony, "Pneumatic System Design Analysis," KSC Collaboration Services, https://sp.ksc.nasa.gov/ne/da/fluids/Fluids%20Wiki/Pneumatic%20System%20Design%20Analysis.aspx.

(7) TRW Systems Group, *Aerospace Fluid Component Designers' Handbook*, Vol. 1, RPL-TDR-64-25, Air Force Rocket Propulsion Laboratory, Edwards Air Force Base, Edwards, California, 1970.

(8) Circle Seal Controls, Engineering Data, Circle Seal, http://www.circle-seal.com/products/technical_data/engdata.pdf, (January 26, 2012).

(9) David G. Gilmore, *Spacecraft Thermal Control Handbook*, Vol. 1: "Fundamental Technologies," American Institute of Aeronautics and Astronautics, Inc., 2002.

(10) Randall F. Barron, *Cryogenic Heat Transfer,* Taylor & Francis, Philadelphia, 1999.

(11) T.M. Flynn, J.W. Draper, and J.J. Roos, "The Nucleate and Film Boiling Curve of Liquid Nitrogen at One Atmosphere," in *Advances in Cryogenic Engineering*, Plenum Press, New York, Vol. 7, 1962, pp. 539–545, Figure 5.

(12) TRW Systems Group, *Aerospace Fluid Component Designers' Handbook*, Vol. 2, RPL-TDR-64-25, Air Force Rocket Propulsion Laboratory, Edwards Air Force Base, Edwards, California, 1970.

This page was intentionally left blank.

APPENDIX C. THERMAL/FLUID DESIGN MARGINS

C.1 Thermal Design Margins for Spacecraft

C.1.1 Design Margins for Passive Systems (Radiators, Insulation, Thermal Storage Devices)

Cryogenic Passive	**Concept**	**30% or PDR**	**60%**	**90% or CDR**
Uncorrelated Model	±17 °C (30.6 °F)	±17 °C (30.6 °F)	±17 °C (30.6 °F)	±17 °C (30.6 °F)
Correlated Model	±11 °C (19.8 °F)	±11 °C (19.8 °F)	±11 °C (19.8 °F)	±11 °C (19.8 °F)
Values are for 95% probability of success.				
Note: Do not use both margins together. Cryogenic design margins shall be used when the temperature will be maintained below 614.67 °R (343.15 K).				

C.1.2 Design Margins for Active Systems (Pumped Fluid Loops, Stored-Coolant Subsystems, Fluids in Motion)

Active Systems	**Concept**	**PDR**	**CDR**	**Qualification**	**Acceptance**
Heat Load Margin	±50%	±45%	±35%	±30%	±25%
Values for cryogenic systems are for 95% probability of success.					

C.1.3 Power Dissipation Design Margins for Heaters

	Concept	**30% or PDR**	**60%**	**90% or CDR**
Power Dissipation	15%	15%	15%	15%
Values are those used in 545-PG-8700.2.1.				

C.2 Thermal Design Margins for Ground Systems

	Concept	30% or PDR	60%	90% or CDR
Surface Temperature Margin	±8.33 °C (15 °F)	±8.33 °C (15 °F)	±2.78 °C (5 °F)	±2.78 °C (5 °F)

or

	Concept	30% or PDR	60%	90% or CDR
Radiation Heat Load Margin	±50%	±45%	±35%	±30%
Convection Heat Load Margin	±50%	±40%	±30%	±15%
Conduction Heat Load Margin	±50%	±40%	±30%	±15%
Note: Do not use both margins together. Use whichever margin challenges the design to the greatest extent.				

C.3 Design Margins for Two-Phase Fluid Quality

If quality (maximum percentage of vapor) is a design requirement, use the following margins.

	Concept	30% or PDR	60%	90% or CDR
Quality Margin	±33%	±33%	±20%	±10%
For example, if the requirement is to provide a maximum of 6% quality, then the system design shall be for 4% quality through the 30% review.				

If quality (maximum percentage of vapor) is required to be zero, then the margin is on subcooling.

	Concept	30% or PDR	60%	90% or CDR
Subcooling	–4.44 °C (8 °F)	–4.44 °C (8 °F)	–3.33 °C (6 °F)	–2.78 °C (5 °F)
Subcooling Temperature Multiplier	2.0	2.0	1.5	1.25
For example, design the system to provide twice the required subcooling, up to the 30% review.				

C.4 Design Margins for Fluid Flow Rate

C.4.1 Incompressible (Liquid) Flow

	Concept	30% or PDR	60%	90% or CDR
Flow Rate Margin	±50%	±50%	±35%	±25%
Note: Apply to nominal flow values.				

C.4.2 Compressible (Gas) Flow

	Concept	30% or PDR	60%	90% or CDR
Flow Rate Margin	±50%	±50%	±30%	±20%
Note: Apply to nominal flow values.				

APPENDIX D. DERIVATION OF EQ. 15

Eq. 15 in 7.6.2 is derived via the Darcy equation:

$$H_L = K\frac{v^2}{2g} \qquad \text{Eq. A}$$

From (3), *Equation 1-16.*

Substituting,

$$\Delta P_R = \rho_R g H_L \qquad \text{Eq. B}$$

As obtained from steady flow energy equation.

and rearranging gives

$$K = \frac{2\Delta P_R}{\rho_R v^2} \qquad \text{Eq. C}$$

Converting velocity to mass flow gives

$$K = \frac{2\Delta P_R}{\rho_R\left(\dfrac{\dot{m}}{\rho_R A}\right)^2} = \frac{2\Delta P_R \rho_R A^2}{\dot{m}^2} \qquad \text{Eq. D}$$

Because the filter flow rate is given in cubic feet per minute at standard conditions (scfm), mass flow must be converted using the ideal gas law with compressibility for standard conditions:

$$Q_{STD} = \frac{\dot{m}}{\rho_{STD}} = \frac{\dot{m}}{\dfrac{P_{STD}}{RT_{STD}Z_{STD}}} = \frac{\dot{m}RT_{STD}Z_{STD}}{P_{STD}} \qquad \text{Eq. E}$$

Substituting Eq. E into Eq. D gives

$$K = \frac{2\Delta P_R \rho_R A^2}{\dfrac{Q_{STD}^2 P_{STD}^2}{R^2 T_{STD}^2 Z_{STD}^2}} = \frac{2\Delta P_R \rho_R A^2 R^2 T_{STD}^2 Z_{STD}^2}{Q_{STD}^2 P_{STD}^2} \qquad \text{Eq. F}$$

Converting rated density to rated pressure and temperature via the ideal gas law with compressibility gives

$$K = \frac{2\Delta P_R \dfrac{P_R}{RT_R Z_R} A^2 R^2 T_{STD}^2 Z_{STD}^2}{Q_{STD}^2 P_{STD}^2} = \frac{2\Delta P_R P_R A^2 R T_{STD}^2 Z_{STD}^2}{Q_{STD}^2 P_{STD}^2 T_R Z_R} \qquad \text{Eq. G}$$

Finally, applying conversion factors and rearranging gives the following:

$$K = \left(\frac{60}{144}\right)^2 \cdot \frac{g_c \pi^2 R P_R \Delta P_R Z_{STD}^2 T_{STD}^2 d_{BL}^4}{8 P_{STD}^2 Q_{STD}^2 Z_R T_R} \qquad \text{Eq. H}$$

which is Eq. 15.

APPENDIX E. KUTATELADZE EQUATION CORRECTION

The following is Randall F. Barron's explanation of the presentation of the Kutateladze equation in his book, *Cryogenic Heat Transfer*. The material was sent by Mr. Barron directly to the KSC Engineering Design Analysis Branch on June 5, 2008. Mr. Barron's work has been typeset and lightly edited for consistency.

Table 11. Comparison of Symbols

Kutateladze	*Cryogenic Heat Transfer*	Kutateladze Equation Units
$\frac{\upsilon}{a}$, Prandtl number of liquid	$\mathrm{Pr}_L = \frac{\mu_L c_L}{k_L}$	dimensionless
υ, kinematic viscosity	$\frac{\mu_L}{\rho_L}$	m^2/s
a, thermal diffusivity	$\frac{k_L}{\rho_L c_L}$	m^2/s
q, boiling heat flux	$\frac{Q}{A_W}$	W/m^2
r, latent heat of vaporization	$i_{fg}\left(\frac{g_c}{g}\right)$	J/kg_f
σ, surface tension	σ_L	kg_f/m
γ, specific weight of liquid	$\frac{\rho_L g}{g_c}$	kg_f/m^3
γ'', specific weight of vapor	$\frac{\rho_G g}{g_c}$	kg_f/m^3
α, boiling coefficient	$h_b = \frac{Q}{A_W \cdot \Delta T}$	$W/m^2 \cdot °C$
λ, thermal cond. of liquid	k_L	$W/m \cdot °C$
$\frac{c \cdot \Delta T}{r}$	$J_a = \frac{c_L \Delta T}{i_{fg}}$, Jakob number	dimensionless
$\frac{p}{\sqrt{\sigma(\gamma - \gamma'')}}$	$K_P = \frac{P_{SAT}}{\sqrt{(g/g_c)\sigma_L(\rho_L - \rho_G)}}$	dimensionless
$(0.44)(10^{-4})^{0.7}$	$6.9735\times10^{-4} \approx 7.0\times10^{-4}$	

NOTE

> Russian scientists often used a "gravimetric" metric system, based on mass (in kilograms [kg]), length (in meters [m]), time (in seconds [s]), and force (in kilograms [kg_f]). The conversion factor between SI and the other metric unit for force is 9.807 newtons per kilogram of force (N/kg_f).

Beginning with the Kutateladze equation in the Kutateladze-notation,

$$\frac{\alpha}{\lambda}\sqrt{\frac{\sigma}{\gamma-\gamma''}} = 0.44\left(\frac{\upsilon}{a}\right)^{0.35}\left[\frac{q}{r\gamma''\upsilon}\sqrt{\frac{\sigma}{\gamma-\gamma''}}\right]^{0.7}\left[\frac{p\times 10^{-4}}{\sqrt{\sigma(\gamma-\gamma'')}}\right]^{0.7}$$

Converting to the notation used in *Cryogenic Heat Transfer* (as given in Table 11), the Kutateladze equation may be written as follows:

$$\frac{(Q/A_W)}{k_L\Delta T}\sqrt{\frac{g_c\sigma_L}{g(\rho_L-\rho_G)}} = 7.0\times 10^{-4}\,\mathrm{Pr}_L^{0.35}\left[\frac{(Q/A_W)\rho_L}{i_{fg}\mu_L\rho_G}\sqrt{\frac{g_c\sigma_L}{g(\rho_L-\rho_G)}}\right]^{0.7}\left[\frac{P}{\sqrt{(g/g_c)(\rho_L-\rho_G)}}\right]^{0.7}$$

Introducing $k_L = \mu_L c_L / \mathrm{Pr}_L$, moving the density ratio (ρ_L/ρ_G) into the second bracketed term, and multiplying and dividing by i_{fg} on the left side yields

$$\frac{\mathrm{Pr}_L\, i_{fg}}{c_L\Delta T}\left[\frac{(Q/A_W)}{i_{fg}\mu_L}\sqrt{\frac{g_c\sigma_L}{g(\rho_L-\rho_G)}}\right] = 0.0007\,\mathrm{Pr}_L^{0.35}\left[\frac{(Q/A_W)}{i_{fg}\mu_L}\sqrt{\frac{g_c\sigma_L}{g(\rho_L-\rho_G)}}\right]^{0.7}\left[\frac{\rho_L P}{\rho_G\sqrt{(g/g_c)(\rho_L-\rho_G)}}\right]^{0.7}$$

Introducing the Jakob number, $J_a = c_L\Delta T / i_{fg}$, on the left side, dividing through by $\mathrm{Pr}_L^{0.35}$, and dividing through by the first bracketed term on the right side yields

$$\frac{\mathrm{Pr}_L^{0.65}}{J_a}\left[\frac{(Q/A_W)}{i_{fg}\mu_L}\sqrt{\frac{g_c\sigma_L}{g(\rho_L-\rho_G)}}\right]^{0.3} = 0.0007\left[\frac{\rho_L P}{\rho_G\sqrt{(g/g_c)(\rho_L-\rho_G)}}\right]^{0.7}$$

Introducing on the right side the definition of the factor K_P, defined by

$$K_P = \frac{P_{SAT}}{\sqrt{(g/g_c)\sigma_L(\rho_L-\rho_G)}}$$

yields

$$\frac{\Pr_L^{0.65}}{J_a}\left[\frac{(Q/A_W)}{i_{fg}\mu_L}\sqrt{\frac{g_c\sigma_L}{g(\rho_L-\rho_G)}}\right]^{0.3} = 0.0007\left[\frac{\rho_L K_P}{\rho_G}\right]^{0.7}$$

Solving for the Jakob number, J_a,

$$\frac{J_a}{\Pr_L^{0.65}} = \frac{1}{0.0007}\left[\frac{(Q/A_W)}{i_{fg}\mu_L}\sqrt{\frac{g_c\sigma_L}{g(\rho_L-\rho_G)}}\right]^{0.3}\left[\frac{\rho_G}{\rho_L K_P}\right]^{0.7}$$

This is the correct form for Equation 4-24, pg. 164, *Cryogenic Heat Transfer*. In the correct form, the factor 0.0007 and K_P shall be in the denominator, instead of the numerator. The equation was written in this form so that the Kutateladze equation could be compared with the Rohsenow equation,

$$\frac{J_a}{\Pr_L^n} = C_{sf}\left[\frac{(Q/A_W)}{i_{fg}\mu_L}\sqrt{\frac{g_c\sigma_L}{g(\rho_L-\rho_G)}}\right]^{1/3}$$

a. In the Kutateladze equation, n = 0.65 for all fluids; in the Rohsenow equation, n = 1 for water and n = 1.7 for all other fluids.

b. In the Kutateladze equation, the exponent on the term containing the heat flux (Q/A_W) is 0.300; in the Rohsenow equation, the corresponding exponent is $^1/_3$ = 0.333.

c. The surface-fluid coefficient C_{sf} in the Rohsenow equation is a constant for a particular surface-fluid combination, independent of the fluid pressure. In the Kutateladze equation, the corresponding factor does not involve the surface-fluid combination; however, there is pressure dependence.

$$\frac{1}{0.0007}\left[\frac{\rho_G\sqrt{(g/g_c)(\rho_L-\rho_G)}}{\rho_L P_{SAT}}\right]^{0.7}$$ corresponds to C_{sf} in the Rohsenow equation.

This is generally not an extremely strong pressure-dependent term, because ρ_G is also pressure-dependent, and the ratio (ρ_G/P_{SAT}) does not vary by orders of magnitude with pressure.

- At 1 atmosphere (atm) = 101.3 kPa (14.69 psia), $(\rho_G/P_{SAT})^{0.7} = (4.604/101.3)^{0.7}$ = 0.1149.

- At 1.349 atm = 136.7 kPa (19.83 psia), $(\rho_G/P_{SAT})^{0.7} = (6.071/136.7)^{0.7}$ = 0.1130.

- At 2 atm = 202.6 kPa (29.38 psia), $(\rho_G/P_{SAT})^{0.7} = (8.753/202.6)^{0.7} = 0.1109$.

For saturated liquid nitrogen boiling at 80 K (–193.2 °C = –315.7 °F = 144 °R), we find the following physical properties:

In *Cryogenic Heat Transfer*	In Kutateladze
Pr_L = 2.14	υ/a = 2.14
(Q/A_W) = 3154 W/m^2 (1000 Btu/hr·ft^2)	q = 3154 W/m^2
i_{fg} = 195.8 kJ/kg (84.2 Btu/lb$_m$)	r = 195.8 kJ/kg$_f$
σ_L = 8.22 mN/m (0.563×10^{-3} lb$_f$/ft)	σ = 0.838×10^{-3} kg$_f$/m
ρ_L = 795.1 kg/m^3 (49.64 lb$_m$/ft^3)	γ = 795.1 kg$_f$/m^3
ρ_G = 6.071 kg/m^3 (0.379 lb$_m$/ft^3)	γ' = 6.071 kg$_f$/m^3
k_L = 0.1362 W/m·°C (0.0787 Btu/hr·ft·°F)	λ = 0.1362 W/m·°C
c_L = 2.063 kJ/kg·°C (0.493 Btu/lb$_m$·°F)	
μ_L = 141 μPa·s (0.341 lb$_m$/ft·hr)	
	υ = 0.1773 mm^2/s
p_{sat} = 136.7 kPa (19.83 psia)	p = 13,939 kg$_f$/m^2
g = 9.807 m/s^2 (32.174 ft/s^2)	g = 9.807 m/s^2
g_c = 1 kg·m/N·s^2 (32.174 lb$_m$·ft/lb$_f$·s^2)	g_c = 9.807 kg$_m$/kg$_f$·s^2

Using these properties, we may calculate the temperature difference, $\Delta T = T_W - T_{SAT}$, for liquid nitrogen in pool boiling at 136.7 kPa (19.83 psia or 1.349 atm) and 80 K (315.67 °F), using the original Kutateladze equation and the form presented in *Cryogenic Heat Transfer* (corrected). We find that these two calculations result in the same temperature difference.

The form presented in *Cryogenic Heat Transfer* separates the term involving ΔT and the term involving (Q/A_W). Because the heat flux term appears (implicitly) in $\alpha = (Q/A_W)/\Delta T$ and also in the first term on the right side, the solution for the heat flux is somewhat more awkward using Kutateladze's original formulation.

Calculation of ΔT – Kutateladze's Original Equation Form

$$\frac{q}{r\gamma''\upsilon}\left(\frac{\sigma}{\gamma-\gamma''}\right)^{1/2}=\frac{(3154)}{(195.8\times10^{3})(6.071)(0.1773\times10^{-6})}\left(\frac{0.838\times10^{-3}}{795.1-6.071}\right)^{1/2} = 15.423$$

$$K_P=\frac{p}{\sqrt{\sigma(\gamma-\gamma'')}}=\frac{13{,}939}{\sqrt{(0.838\times10^{-3})(795.1-6.071)}} = 17{,}140$$

The left side of the original Kutateladze equation is a form of a "boiling Nusselt number,"

$$\frac{\alpha}{\lambda}\sqrt{\frac{\sigma}{\gamma-\gamma''}}=(0.44)(2.14)^{0.35}(15.423)^{0.7}(17{,}142\times10^{-4})^{0.7} = 5.6840$$

The boiling heat transfer coefficient is

$$\alpha=\frac{(5.6840)(0.1362)}{\sqrt{(0.838\times10^{-3})/(795.1-6.071)}}=\frac{(5.6840)(0.1362)}{(0.0010306)} = 751.2\ \text{W/m}^2\cdot{}^\circ\text{C} = \frac{(Q/A_W)}{\Delta T}$$

The temperature difference, according to the original Kutateladze equation, is

$$\Delta T=\frac{3154}{751.2} = 4.20\ {}^\circ\text{C} = T_W - T_{SAT} \Leftarrow$$

Calculation of ΔT – Kutateladze's Equation in *Cryogenic Heat Transfer* Form

$$\frac{(Q/A_W)}{i_{fg}\mu_L}\sqrt{\frac{g_c\sigma_L}{g(\rho_L-\rho_G)}}=\frac{(3154)}{(195.8\times10^{3})(141\times10^{-6})}\sqrt{\frac{(1)(8.22\times10^{-3})}{(9.807)(795.1-6.071)}} = 0.11775$$

$$K_P=\frac{P_{SAT}}{\sqrt{(g/g_c)\sigma_L(\rho_L-\rho_G)}}=\frac{(136.7\times10^{3})}{\sqrt{(9.807/1)(8.22\times10^{-3})(795.1-6.071)}} = 17{,}140$$

The Jakob number is

$$J_a=\frac{(2.14)^{0.65}}{(0.0007)}(0.11775)^{0.3}\left[\left(\frac{6.071}{795.1}\right)\frac{1}{17{,}140}\right]^{0.7}=0.04417=\frac{c_L\Delta T}{i_{fg}}$$

$$\Delta T=\frac{(0.04417)(195.8\times10^{3})}{(2.063\times10^{3})} = 4.20\ {}^\circ\text{C} \Leftarrow$$

For comparison, we can determine the temperature difference ΔT using the Rohsenow equation for nucleate boiling:

$$\frac{J_a}{\mathrm{Pr}_L^{1.7}} = C_{sf}\left[\frac{(Q/A_w)}{i_{fg}\mu_L}\sqrt{\frac{g_c\sigma_L}{g(\rho_L-\rho_G)}}\right]^{1/3}$$

Using a value of C_{sf} = 0.013, we find the Jakob number, according to the Rohsenow equation:

$J_a = (0.013)(2.14)^{1.7}\,(0.11775)^{1/3} = 0.02323$

The temperature difference is

$$\Delta T = \frac{(0.02323)(195.8)}{(2.063)}$$ = 2.20 °C (compared to 4.20 °C from the Kutateladze equation)

The experimentally measured temperature difference for liquid nitrogen with a boiling heat flux of (Q/A_W) = 3154 W/m^2 = 0.3154 W/cm^2 is ΔT = 3.2 °C.

See (11).

The differences between calculated and experimental values are

- (4.2 °C – 3.2 °C)/(3.2 °C) = +31% (for the Kutateladze equation) and
- (2.2 °C – 3.2 °C)/(3.2 °C) = –31% (for the Rohsenow equation).

STANDARDIZATION DOCUMENT IMPROVEMENT PROPOSAL

INSTRUCTIONS

1. The preparing activity must complete blocks 1, 2, 3, and 8. In block 1, both the document number and revision letter should be given.
2. The submitter of this form must complete blocks 4, 5, 6, and 7.
3. The preparing activity must provide a reply within 30 days from receipt of the form.

NOTE: This form may not be used to request copies of documents, nor to request waivers or clarification of requirements on current contracts. Comments submitted on this form do not constitute or imply authorization to waive any portion of the referenced document or to amend contractual requirements.

I RECOMMEND A CHANGE:	1. DOCUMENT NUMBER KSC-STD-Z-0017	2. DOCUMENT DATE May 8, 2014

3. DOCUMENT TITLE
Engineering Analysis, Thermal/Fluid,
Standard For

4. NATURE OF CHANGE *(Identify paragraph number and include proposed rewrite, if possible. Attach extra sheets as needed.)*

5. REASON FOR RECOMMENDATION

6. SUBMITTER

a. NAME *(Last, First, Middle Initial)*	b. ORGANIZATION	
c. ADDRESS *(Include Zip Code)*	d. TELEPHONE *(Include Area Code)*	7. DATE SUBMITTED

8. PREPARING ACTIVITY

a. NAME	b. ORGANIZATION
Craig Fortier	Engineering Design Analysis Branch

c. ADDRESS *(Include Zip Code)*
Mail Stop NE-M1, Kennedy Space Center, Florida 32899